PHYSICAL REVIEW A VOLUME 38, NUMBER 4 AUGUST 15, 1988

Instability in injected-laser and optical-bistable systems

Hu Gang
Center of Theoretical Physics, Chinese Center of Advanced Science and Technology (World Laboratory), Beijing, China and Department of Physics, Beijing Normal University, Beijing, China

Yang Guo-jian
Department of Physics, Beijing Normal University, Beijing, China
(Received 30 November 1987)

An analytical function is derived which can serve as a criterion of the instability boundary of both optical-bistable (OB) systems and laser systems with an injected coherent signal (LIS). By means of the criterion, we analyze, in various asymptotic limits, the instability regions of OB and LIS in the parameter space. In both good- and bad-cavity conditions of LIS a full hysteresis loop between coexisting stable states is observed for the first time.

I. INTRODUCTION

The study of optical systems exhibiting bistability[1,2] and laser oscillators driven by an external coherent field[3,4] has been a very active field in the last two decades. Recently, the instability manifested by optical bistability (OB) and by lasers with an injected signal (LIS) has attracted much attention.[5–11] It has been found that a large variety of behaviors, such as quasiperiodicities, unstable pulsations, and chaos, may appear in the regions where instability functions. The theoretical and practical importance of such kinds of erratic behavior has been repeatedly emphasized.

A number of publications have contributed to showing the instability as well as the numerous bifurcations in the instability regions of OB and LIS by taking various combinations of parameters.[12–15] Moreover, many kinds of approximations have been used to reduce the complex initial Maxwell-Bloch equations to lower dimensions. However, to date, no result about the global structure of the instability regions of OB and LIS has been reported. The reason is that, on the one hand, the Maxwell-Bloch equations are essentially multidimensional, and on the other hand, there are so many parameters involved in the problem.

Lugiato *et al.* shed much new light on the understanding of the instability problem. They analyzed the boundaries of the instability regions of OB and LIS in the Gaussian radial distribution approximation[16] and in the plane-wave approximation.[17] Nevertheless, still only a small part of the parameter space has been examined since the mathematical form suggested for determining the instability boundary is implicit. In Refs. 18 and 19 the instability condition of OB in the limit of large small-signal gain was given explicitly.

The main purpose of the present paper is to suggest an explicit criterion in terms of which a description of the global structure of the instability regions of OB and LIS in the parameter space becomes available. The publication is organized as follows. In Sec. II we present the model and the general theory defining the explicit criterion function of instability boundary. In Sec. III, in terms of the criterion function, the instability boundary of OB in various limiting cases are specified. Section IV contributes to the discussion of the instability of LIS. In Sec. V we summarize the results and indicate various applications and extensions of our theory.

It is emphasized that in the presentation we focus on the formulation of the instability boundary. We do not proceed further into detail about what happens in the instability regions, though we are sure that various erratic behaviors can emerge only in these regions.

II. GENERAL THEORY

A. Optical bistability

We consider an optical undirectional ring cavity filled with a passive medium, consisting of homogeneously broadened two-level atoms, and driven by an external coherent optical signal. Considering only the single-mode case, applying the plane wave approximation, and taking the mean-field limit, we can reduce the Maxwell-Bloch equations to[20]

$$\begin{aligned} \dot{x} &= -k[(1+i\theta)x - y + 2Cp] , \\ \dot{p} &= xD - (1+i\Delta)p , \\ \dot{D} &= -\gamma[(x^*p + xp^*)/2 + D - 1] , \end{aligned} \tag{2.1}$$

where all the variables and the parameters are dimensionless. x and p, being proportional to the output field and the atomic polarization, are complex numbers, while the normalized atomic population D is real and positive. Then the equations are essentially five dimensional. The system parameters C, k, and γ designate the small-signal gain, the cavity linewidth, and the atomic population decay rate, respectively. Both k and γ are scaled to the homogeneous linewidth $\gamma_\perp$. Given the frequencies of the external field, the atoms, and the cavity as ω_0, ω_A, and ω_c, respectively, we scale the atomic detuning and the cavity mistuning as $\Delta = (\omega_A - \omega_0)/\gamma_\perp$ and $\theta = (\omega_c - \omega_0)/(k\gamma_\perp)$. Therefore there are six independent parameters (C, k, γ, θ, Δ, and y) involved in the problem. The incident field y is taken to be positive. It seems to be an extremely difficult task to clarify the instability problem of five-dimensional coupled nonlinear differential equations in a six-dimensional parameter space.

In spite of the nonlinearity of the coupled equations, the explicit stationary solutions of Eqs. (2.1) can be worked out,

$$\begin{aligned} y &= |x_s| \{[1+2C/(1+\Delta^2+|x_s|^2)]^2+[\theta-2\Delta C/(1+\Delta^2+|x_s|^2)]^2\}^{1/2} , \\ D_s &= (1+\Delta^2)/(1+\Delta^2+|x_s|^2) , \\ p_s &= (1-i\Delta)x_s/(1+\Delta^2+|x_s|^2) . \end{aligned} \tag{2.2}$$

Based on the explicit solutions, one may apply linear stability analyses and, in principle, reveal the instability regions. The equations of the linearizations of Eqs. (2.1) about the steady state (2.2) turn out to be

$$\begin{bmatrix} \delta\dot{x} \\ \delta\dot{x}^* \\ \delta\dot{p} \\ \delta\dot{p}^* \\ \delta\dot{D} \end{bmatrix} = \begin{bmatrix} -k(1+i0) & 0 & -2Ck & 0 & 0 \\ 0 & -k(1-i\theta) & 0 & -2Ck & 0 \\ D_s & 0 & -(1+i\Delta) & 0 & x_s \\ 0 & D & 0 & -(1-i\Delta) & x_s^* \\ -\gamma p_s^*/2 & -\gamma p_s/2 & -\gamma x_s^*/2 & -\gamma x_s/2 & -\gamma \end{bmatrix} \begin{bmatrix} \delta x \\ \delta x^* \\ \delta p \\ \delta p^* \\ \delta D \end{bmatrix} , \tag{2.3}$$

with

$$x = x_s+\delta x, \quad p = p_s+\delta p, \quad D = D_s+\delta D , \tag{2.4}$$

which lead to the characteristic equation

$$\lambda^5+a_1\lambda^4+a_2\lambda^3+a_3\lambda^2+a_4\lambda+a_5=0 , \tag{2.5}$$

where

$$\begin{aligned} a_1 &= 2k+\gamma+2 , \\ a_2 &= k^2(1+\theta^2)+(2\gamma+1+\Delta^2+\gamma x^2)+2k(\gamma+2) \\ &\quad +4kCD , \\ a_3 &= \gamma(1+\Delta^2+x^2)+2k(2\gamma+1+\Delta^2+\gamma x^2) \\ &\quad +k^2(1+\theta^2)(\gamma+2) \\ &\quad +4kCD(\gamma+k+1)-C\gamma k(p^*x+px^*) , \end{aligned} \tag{2.6a}$$

$$\begin{aligned} a_4 &= 2k\gamma(1+\Delta^2+x^2)+k^2(1+\theta^2)(2\gamma+1+\Delta^2+\gamma x^2) \\ &\quad +2kCD[2k(1-\Delta\theta)+2\gamma(k+1)+\gamma x^2] \\ &\quad +Ck\gamma[i(\Delta+k\theta)(p^*x-px^*) \\ &\qquad -(k+1)(p^*x+px^*)]+4k^2C^2D^2 , \\ a_5 &= \gamma k^2\{4C^2D[D-(p^*x+px^*)/2] \\ &\qquad +(1+\theta^2)(1+\Delta^2+x^2)+4CD(1-\Delta\theta)\} . \end{aligned}$$

Here and henceforth we replace p_s, p_s^*, D_s, and $|x_s|^2$ simply by p, p^*, D, and x^2, respectively. Considering

$$\begin{aligned} i(p^*x-px^*) &= -2\Delta x^2/(1+\Delta^2+x^2) , \\ (p^*x+px^*) &= 2\Delta x^2/(1+\Delta^2+x^2) , \end{aligned} \tag{2.6b}$$

and having D provided in Eqs. (2.2), all the coefficients in (2.6a) are presented explicitly in terms of the six parameters C, k, γ, Δ, θ, and x^2. (Here it is convenient to employ x^2 instead of y as an independent parameter.)

It is, obviously, impossible to solve Eq. (2.5) analytically and obtain explicit solutions of the eigenvalues. However, a general discussion about the instability of the steady solutions (2.2) may be possible without seeking the precise solutions of λ. By the Routh-Hurwits criterion[21] one may clarify the instability conditions. However, the many inequalities provided there are not convenient for specifying the instability boundary in the space of control parameters. Therefore, we proceed in the following way. First, some necessary conditions for (2.2) to be stable are

$$a_1,a_2,a_3,a_4>0 , \tag{2.7a}$$

$$a_5>0 . \tag{2.7b}$$

The steady state may lose its stability via Hopf bifurcation. Assume, at the critical situation, we have

$$\lambda=i\nu, \quad \nu>0 . \tag{2.8}$$

Substituting λ in (2.5) by (2.8), a pair of equations are justified,

$$\nu^4-a_2\nu^2+a_4=0 , \tag{2.9a}$$

$$a_1\nu^4-a_3\nu^2+a_5=0 . \tag{2.9b}$$

According to the requirement that (2.9a) and (2.9b) must, at least, have an identical solution, we may transform Eqs. (2.9) to

$$\begin{aligned} (a_2-\nu^2)/(a_3/a_1-\nu^2) &= a_1a_4/a_5 , \\ (a_2-a_3/a_1)\nu^2 &= a_4-a_5/a_1 , \end{aligned} \tag{2.10}$$

leading to the critical condition of Hopf bifurcation,

$$f = (a_1a_2-a_3)(a_3a_4-a_2a_5)-(a_1a_4-a_5)^2=0 . \tag{2.11}$$

In fact, it is easy to verify that

$$f > 0 \tag{2.12}$$

is one more necessary condition for the stability of (2.2). It is emphasized that Eqs. (2.7) and (2.12) are only necessary conditions for the stable steady solutions. They are not sufficient. For instance, it is possible that Eq. (2.5) has two pairs of conjugate complex roots with positive real parts and one negative real root in the case of $a_1, \ldots, a_5, f > 0$. At any rate, the violation of any condition of Eqs. (2.7) and (2.12) provides a sufficient condition for the instability of the steady state.

There are two points worth noting to this end.

(i) All the necessary conditions of Eqs. (2.7) and (2.12) are not equally important. Starting from a stable region and varying the parameters continuously, there are only two possibilities to alter the stability of the system. First, one eigenvalue passes the origin, or second, a pair of conjugate complex eigenvalues cross the imaginary axis. In the former case a_5 changes its sign first while in the latter case it is f that first alters its sign. In any case, anyone among a_1, a_2, a_3, and a_4 can never be the first one turning negative as the system crosses the instability boundary. Therefore a_1, a_2, a_3, and a_4 have no relation with the boundary condition of instability. Only the critical conditions $a_5=0$ and $f=0$ can serve to define the instability boundary. Moreover, one may easily verify that

$$d(y^2)/d(x^2) \propto a_5 \ .$$

Hence, $a_5<0$ represents, in y-x space, the segment of the solutions with a negative slope that we are not concerned with. We are interested only by the solutions with a positive slope. Hence forward, when we talk about instability we always mean positive-slope instability, i.e., the stability on the branches where $a_5>0$. Thus among so many (six) necessary conditions only the unique condition (2.11) is essential for the instability boundary. (By the Routh-Hurwits criterion one should consider five inequalities, none of which can be regarded as the most important one.)

(ii) Though Eqs. (2.7) and (2.12) are not sufficient for (2.2) to be stable, one may identify the stability of the steady solutions in many practical cases. Before proceeding further let us give a definition of connected regions. Region A and region B are regarded as connected if and only if one may pass from one to the other via any path, by varying the parameters continuously and retaining the signs of $a_1, \ldots, a_5$ and f through the whole path. It is obvious that a region connected with a stable region must be stable. In many simple cases one may easily justify the stability of the solutions (e.g., as $x^2 \to \infty$ or as $\Delta=\theta=0$). Thus in some complex situations it might be possible to verify the stability of the solutions by proving the connection of the given regions with certain known stable regions. This procedure will be shown to be powerful in many practical cases. Together with a proof of the connection, Eq. (2.12) can serve as both a necessary and sufficient condition for the stationary solutions to be stable. The instability boundary is given by Eq. (2.11).

The condition for the instability boundary has been analyzed by Lugiato *et al.* Up to Eqs. (2.9), our approach is only slightly different from their method [cf. Refs. 16 and 17]. In fact, Eqs. (2.9) are essentially the same as Eqs. (3.15) in Ref. 17. However, in Ref. 17, ν appears in a pair of equations in an complicated way that led the authors to conclude that in most cases an analytical form for the elimination of ν is not available.[17] The simple form of Eqs. (2.9) leads us to the opposite conclusion: In any case (apart from $\nu=0$, which indicates $a_5=0$) an analytical elimination of ν can be realized easily.

From Eqs. (2.5)–(2.12), the mathematical procedures need only an elementary calculation and a little trick. However, from the physical point of view, we have carried out an extremely important jump. The physical impacts of the realization of Eq. (2.12) can be noted as follows.

(1) For the first time, we obtain an analytical and explicit criterion defining the instability boundary. Previously, various asymptotic limits have been used individually to detect instability basins by chance. Now all these limits can be studied together in terms of a single function f.

(2) Equation (2.12) is exact, and no further approximations reducing the dimension of the variable space are needed.

(3) The function f can be regarded as a potential. Instability may arise in all the basins where the value of the potential is less than zero. Then by studying the level curves of equal potential and the basin structure of the function f it becomes possible to predict the global structure of the instability regions.

(4) Moreover, the new approach can be directly extended to many practical situations which will be cited in Sec. V.

B. Laser with a coherent external optical signal

With the same approximations stated for OB, we may drive the Maxwell-Bloch equations[9]

$$\begin{aligned} \dot{x} &= -k[1+i\delta)x - y + 2Cp] \ , \\ \dot{p} &= xD - (1+i\Delta)p \ , \\ \dot{D} &= -\gamma[(x^*p + xp^*)/2 + D + 1] \ ; \end{aligned} \tag{2.13}$$

Eqs. (2.13) are identical to Eqs. (2.1) apart from $D+1$ replacing $D-1$ in the last equation. The difference indicates that now the medium is active rather than passive. The steady solutions of (2.13) read

$$y = |x_s| \{[1-2C/(1+\Delta^2+|x_s|^2)]^2 + [\theta+2\Delta C/(1+\Delta^2+|x_s|^2)]^2\}^{1/2} \ , \tag{2.14}$$

and

$$D_s = -(1+\Delta^2)/(1+\Delta^2+|x_s|^2) \ ,$$

$$p_s = -(1-i\Delta)x_s/(1+\Delta^2+|x_s|^2) \ .$$

Replacing Eq. (2.6b) by

$$\begin{aligned} i(p^*x - px^*) &= 2\Delta x^2/(1+\Delta^2+x^2) \ , \\ (p^*x + px^*) &= -2x^2/(1+\Delta^2+x^2) \ , \end{aligned} \tag{2.15}$$

and D by Eq. (2.14), Eqs. (2.6a), (2.7), and (2.12) make sense in the case of LIS.

To conclude this section we present three figures, which may provide some intuitive information about the function f. In Figs. 1 and 2 we use the parameters taken by Lugiato *et al.* in Ref. 16. The perfect coincidence of the segments of negative f in our case with the instability regions denoted in Ref. 16 is evident. In Fig. 3 we find that the function f falls down into negative regions twice. We predict that in region 2 an instability island which is, generally, not easy to find in LIS must exist.

III. INSTABILITY OF OB

In this section and the following sections we focus on the instability problem in various asymptotic limits, which include most previous results of instability as special cases. In the presentation, most limiting cases are realizable and of practical interest, while some of them may not be physically meaningful. Nevertheless, an understanding of all the limiting cases must be theoretically useful for clarifying the global structure of the instability regions in the parameter space.

A. $\Delta=\theta=0$

Now we consider purely absorptive OB. Equations (2.3) can be separated into two independent sets of equations:

$$\begin{bmatrix} \delta\dot{x} \\ \delta\dot{p} \\ \delta\dot{D} \end{bmatrix} = \begin{bmatrix} -k & -2kC & 0 \\ D_s & -1 & x_s \\ -\gamma p_x & -\gamma x_s & -\gamma \end{bmatrix} \begin{bmatrix} \delta x \\ \delta p \\ \delta D \end{bmatrix}, \tag{3.1a}$$

$$\begin{bmatrix} \delta\dot{\bar{x}} \\ \delta\dot{\bar{p}} \end{bmatrix} = \begin{bmatrix} -k & -2kC \\ D_s & -1 \end{bmatrix} \begin{bmatrix} \delta\bar{x} \\ \delta\bar{p} \end{bmatrix}, \tag{3.1b}$$

with all variables in set (3.1a) being real while those in (3.1b) are imaginary. In (3.1b) the steady solution

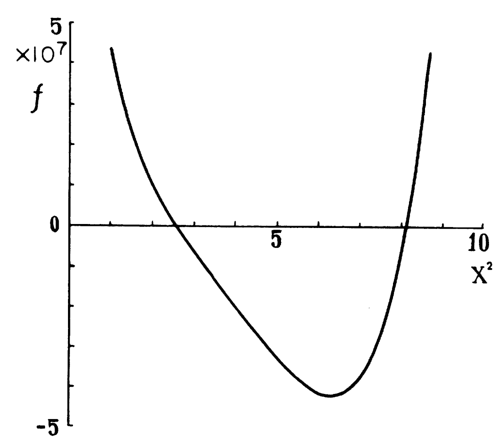

FIG. 1. Optical bistability. Function f, defined in (2.11), plotted against $|x|^2$. The parameters are chosen as $C=75$, $k=0.5$, $\gamma=2$, $\theta=-9$, and $\Delta=1$, which were used in Fig. 4(a) of Ref. 16. The region of negative f is perfectly identical to the unstable segment in Ref. 16.

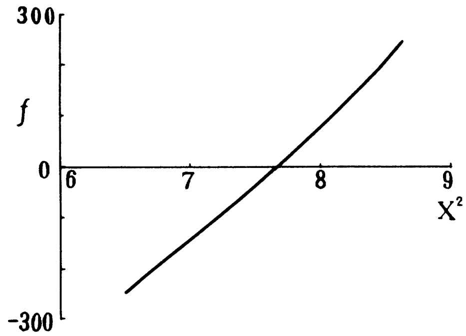

FIG. 2. Laser with an injected signal. f is plotted against $|x^2|$. Parameters used are $C=20$, $k=0.5$, $\gamma=0.05$, $\theta=2$, and $\Delta=1$, which were used in Fig. 6(a) of Ref. 16. The validity of (2.12) is justified.

$\delta\bar{x}=\delta\bar{p}=0$ is always stable. Thus the linearization of Eqs. (2.1) is essentially three dimensional. Instead of Eqs. (2.7) and (2.12), we now have

$$b_1, b_2, b_3 > 0 \tag{3.2a}$$

and

$$f=b_1 b_2 - b_3 > 0 \tag{3.2b}$$

as the stability conditions of the steady solutions, where

$$\begin{aligned} b_1 &= k+\gamma+1 , \\ b_2 &= k+\gamma+k\gamma+\gamma x_s^2+2kCD_s , \\ b_3 &= k\gamma+2k\gamma CD_s+k\gamma x_s^2-2k\gamma Cp_s x_s^2 . \end{aligned} \tag{3.3}$$

Unlike Eqs. (2.7) and (2.12), the conditions (3.2) are both necessary and sufficient for the stability of the solutions

$$y=x_s[1+2C/(1+x_s^2)] . \tag{3.4}$$

It is easy to check that

$$b_1, b_2, f > 0$$

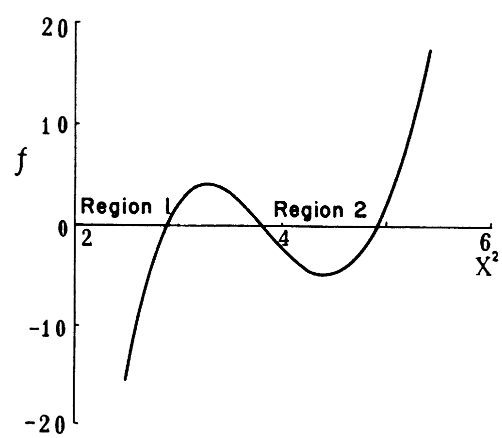

FIG. 3. Laser with an injected signal. Parameters used are $C=20$, $k=0.1$, $\gamma=0.01$, $\theta=-5$, and $\Delta=5$. f falls into the negative region twice. In region 2 an instability island may be expected.

Hence, the steady solutions (3.4) must be stable in the region $b_3>0$. The condition $b_3<0$ represents the negative-slope branch in the triple-valued state equations. Therefore the global structure of the instability region in the full resonance case is completely clarified. In fact, the purely absorptive OB is a well-known model. Our result is not new. However, here we apply our new approach to this simplest case and the result is an elementary part of the forthcoming rich and general results.

B. $x^2 \gg k,\gamma,\Delta,\theta,C=O(1)$

In the asymptotic limit we have

$$a_1=2k+\gamma+2,\quad a_2=\gamma x^2,\quad a_3=\gamma(1+2k)x^2 ,$$
$$a_4=k\gamma[2+k(1+\theta^2)]x^2,\quad a_5=k^2\gamma(1+\theta^2)x^2 \tag{3.5}$$

(Here and henceforth, we use the sign of equality whenever it is valid in the leading order.) It is apparent that $a_1,\ldots,a_5>0$. A direct calculation shows

$$f=(a_1a_2-a_3)(a_3a_5-a_2a_5)\gg 1 . \tag{3.6}$$

These results are consistent with the conclusion that the steady state should be stable as $x^2\to\infty$ (i.e., $y\to\infty$) since then the system must be completely controlled by the external driven field.

With two stable samples ($\Delta=\theta=0$ and $x^2\to\infty$) in hand we may confirm the stability properties in more complicated situations by considering the connections. We put most of results in Table I. In Table I the site $(A,\bar{B})$ means the limit

$$A\gg\bar{B}\gg\text{other parameters}=O(1) . \tag{3.7}$$

The results can be summarized as follows.

(i) In all the sites denoted by "2," the system is stable and single valued. All these regions are connected with the region $x^2\gg 1$.

(ii) All the regions denoted by "1" are connected with the region $\Delta=\theta=0$, and then the solutions with positive slope are always stable.

Apart from cases 1 and 2, there remain few limits in Table I. We will show that the limits $k\gg\gamma\gg 1$ and $\gamma\gg k\gg 1$ give the same instability boundary. Thus we denote them together by "3." Now let us study cases 3, 4, and 5 in detail, and leave the simplest cases (1 and 2) for readers to check by themselves. Here we only remind readers of the following. If the limit $C\gg 1$ is taken, the upper and the lower branches should be distinguished. The upper branch covers the domain

$$x^2>2C[(1+\Delta^2)(1+\theta^2)]^{1/2} \tag{3.8}$$

while the lower branch covers

$$1+\Delta^2>x^2>0 . \tag{3.9}$$

C. $k\gg 1$

This is a very bad cavity condition. The coefficients of Eq. (2.5) can be specified as

TABLE I. The stability properties of OB in various limiting cases. The site $(A,\bar{B})$ means the limit $A\gg\bar{B}\gg 1$. The regions denoted by "1" are connected with the region $\Delta=\theta=0$, and the regions denoted by "2" are connected with the region $x^2\gg 1$. The stability behavior in regions 3, 4, and 5 is described in Secs. III C–III E, respectively. In the last column, the letters u and l represent the words upper and lower, respectively.

	$1/k$	k	$1/r$	r	Δ^2	θ^2	$1/C$	C	
								u	l
$1/k$			1	1	2	2	2	1	1
k			1	3	2	2	2	4	1
$1/r$	1	1			2	2	2	4	1
r	1	3			2	2	2	4	5
Δ^2	2	2	2	2		2	2	1	1
θ^2	2	2	2	2	2		2	4	1
$1/C$	2	2	2	2	2	2			
C	1	1	1	4	2	2			

$$a_1=2k,\quad a_2=(1+\theta^2)k^2$$
$$a_3=(1+\theta^2)(\gamma+2)k^2+4k^2CD ,$$
$$a_4=[(1+\theta^2)(2\gamma+1+\Delta^2+\gamma x^2)+4CD(1-\Delta\theta)+4\gamma CD-2\gamma C(1+\Delta\theta)x^2/(1+\Delta^2+x^2)+4C^2D^2]k^2 , \tag{3.10}$$
$$a_5=\gamma k^2\{4C^2D[D-(p^*x+px^*)/2]+(1+\theta^2)(1+\Delta^2+x^2)+4C(1+\Delta^2)(1-\Delta\theta)/(1+\Delta^2+x^2)\} .$$

Equation (2.11) can be simplified to

$$f=a_1a_2(a_3a_4-a_2a_5)\propto a_3a_4-a_2a_5 . \tag{3.11}$$

The sign of f depends on the concrete values of C, Δ, θ, γ, and x^2. The situation becomes complex as well as interesting. Equation (3.11) can be analyzed thoroughly. However, in the present paper we prefer to require further limits to simplify the formula even more rather than proceeding to a general analysis.

Besides the limit $k\gg 1$, let us consider a further limit

$$k\gg\gamma\gg 1 .$$

Now a_3 and a_4 in Eqs. (3.10) can be further reduced to

$$a_3=\gamma(1+\theta^2)k^2 ,$$
$$a_4=\gamma k^2\left[(1+\theta^2)(2+x^2)+4CD-\frac{2C(1+\Delta\theta)x^2}{(1+\Delta^2+x^2)}\right] , \tag{3.12}$$

and then

$$f\propto(a_3a_4-a_2a_5\propto a_3a_4\propto a_4 . \tag{3.13}$$

The sign of f is identical to that of a_4. The necessary and sufficient condition for the stability of the steady state is

$a_4 > 0$, namely,

$$x^2(1+\Delta\theta) < \left[(1+\theta^2)(2+x^2)(1+\Delta^2+x^2) + \frac{4C(1+\Delta^2)}{(2C)} \right] . \quad (3.14)$$

[It is obvious that one may reach the parameter region where (3.14) is valid, starting from the region $\theta=\Delta=0$, by fixing x^2 and C and retaining the signs of a_1, a_2, a_3, a_4, and f via the path in the Δ-θ plane $(0,0)\to(0,\theta)\to(\Delta,\theta)$. Thus the parameter region (3.14) must be connected with the region $\Delta=\theta=0$ so far as the solutions with a positive slope are considered.] With (3.14) one may describe the instability boundary in C-Δ-θ-x space. Here we restrict ourselves to the following conclusions.

(i) A direct verification shows that positive-slope instability can never be observed in the entire region $\Delta\theta<0$ (i.e., in the second and fourth quadrants and on the θ and Δ axes in the Δ-θ parameter plane).

(ii) For small C (for instance, $C<2$), (3.14) is always valid, and then one can never find instability.

(iii) For large C and in the upper branch, where we have, approximately, $x^2 > 2C[(1+\Delta^2)/(1+\theta^2)]^{1/2}$ [cf. Eq. (3.8)], Eq. (3.14) is valid identically. The entire upper branch is stable.

(iv) For large C and in the lower branch, Eq. (3.14) can be replaced by

$$x^2(1+\Delta\theta) < 2(1+\Delta^2) . \quad (3.15)$$

According to (3.9) and (3.15), the condition under which instability arises in the lower branch can be specified as

$$(1+\Delta\theta) > 2 ,$$

leading to

$$\Delta\theta > 1 . \quad (3.16)$$

In this case instability always first appears near the turning point. The segment near $x^2=0$ is always stable.

D. $\gamma \gg 1$

In this asymptotic case Eqs. (2.6a) reduce to

$$a_1=\gamma, \quad a_2=(2+x^2+2k)\gamma$$

$$a_3=[(1+\Delta^2+x^2)+4k+2kx^2(1+\theta^2) +4kCD-2kCx^2/(1+\Delta^2+x^2)]\gamma ,$$

$$a_4=[2k(1+\Delta^2+x^2)+k^2(1+\theta^2)(2+x^2) +4kCD(k+1) -2k^2C(1+\Delta\theta)x^2/(1+\Delta^2+x^2)]\gamma . \quad (3.17)$$

Equation (2.12) can be written as

$$f=a_1a_2(a_3a_4-a_2a_5)-(a_1a_4)^2>0 . \quad (3.18)$$

In the limit $\gamma \gg k \gg 1$, a_2, a_3, and a_4 can be further simplified to

$$a_2=2k\gamma, \quad a_3=k^2(1+\theta^2) ,$$

$$a_4=\gamma k^2[(1+\theta^2)(2+x^2)+4CD -2C(1+\Delta\theta)/(1+\Delta^2+x^2)] .$$

Equation (3.18) can be reduced to

$$f=a_1a_2a_3a_4 \propto a_4 > \theta ,$$

which is exactly the same as Eq. (3.13). Then the limits $\gamma \gg k \gg 1$ and $k \gg \gamma \gg 1$ give the same instability boundary. Thus both of them are denoted by "3" in Table I. Generally, the limits $A \gg B \gg 1$ and $B \gg A \gg 1$ may provide rather different instability behaviors. (For instance, the instability boundary in the limit $C \gg k \gg 1$ is completely different from that in the limit $k \gg C \gg 1$.)

Let us study the case $\gamma \gg C \gg 1$. Now one should distinguish the upper and lower branches.

In the upper branch, Eq. (3.8) is valid, and then we can reduce (3.17) to

$$a_2=\gamma x^2, \quad a_3=[(1+2k)x^2-2kC]\gamma ,$$

$$a_4=[2kx^2+k^2(1+\theta^2)x^2-2k^2C(1+\Delta\theta)]\gamma , \quad (3.19)$$

$$a_5=\gamma k^2[-4C^2(1+\Delta^2)/x^2+(1+\theta^2)x^2] .$$

Equation (3.18) may be replaced by

$$f \propto a_3a_4-a_2a_5>0 , \quad (3.20)$$

where a_1, a_2, and a_4 are, obviously, not negative. A sufficient condition for the turning point ($a_5=0$) to be unstable is

$$a_3=(1+2k)[(1+\Delta^2)/(1+\theta^2)]^{1/2}-k<0 ,$$

producing

$$(1+\theta^2) > (1+\Delta^2)(2+1/k)^2 . \quad (3.21)$$

It is possible that instability may first appear far away from the turning point. In this case, a more precise instability boundary in the upper branch can be drawn by directly employing Eq. (3.20).

In the lower branch, Eq. (3.19) should be replaced by

$$a_2=(2+x^2+2k)\gamma ,$$

$$a_3=[4kCD-2kCx^2/(1+\Delta^2+x^2)]\gamma ,$$

$$a_4=[4kCD(k+1)-2k^2C(1+\Delta\theta)x^2/(1+\Delta^2+x^2)]\gamma , \quad (3.22)$$

$$a_5=4\gamma k^2C^2D(1+\Delta^2-x^2)/(1+\Delta^2+x^2) .$$

Now in the leading order the form of the function f reads

$$f=a_1a_2(a_3a_4-a_2a_5)-(a_1a_4)^2 ,$$

which is still complex. However, at the turning point of the lower branch ($x^2=1+\Delta^2$ and $a_5=0$), the instability condition can be greatly simplified as

$$f \propto a_4(a_2a_3-a_1a_4) =\gamma^3k^2C^2(k+2-k\Delta\theta)(k+1+\Delta^2+k\Delta\theta)<0 , \quad (3.23)$$

which yields

$$\Delta\theta > 1+2/k \quad (3.24)$$

or

$$\Delta\theta < -(1+1/k+\Delta^2/k) \ . \quad (3.25)$$

Equation (3.24) is identical to Eq. (3.16) as $k>>1$. According to (3.25), Δ and θ must be in the second or fourth quadrants ($\Delta\theta<0$) and the absolute minimal value of θ is

$$\theta > 2\sqrt{1+k}\ /k \ . \quad (3.26)$$

Equations (3.24) and (3.25) as well as (3.21) serve merely as sufficient conditions for the instability of the lower branch and the upper branch, respectively, since in both cases only the turning points have been taken into account. However, in many circumstances, instability arises first at the turning points, then Eqs. (3.24), (3.25), and (3.21) may be used to define the instability boundary. The region (3.25) is denoted by "4" in Table I.

E. $C \gg 1$

First, let us discuss what happens in the upper branch. It is surprising that apart from replacing $a_1=\gamma$ by $a_1=2k+2+\gamma$ (now we do not take the limit $\gamma\gg 1$), we completely recover (3.19). Since the positive number a_1 does not affect the instability boundary, Eqs. (3.20) as well as (3.21) make sense in the single limit $C\gg 1$. An interesting conclusion is that for the large value of the bistability parameter C, the instability boundary in the upper branch is almost independent of γ, the ratio of the longitudinal atomic decay rate to the transversal one.

Figure 4 shows the instability boundary in Δ-θ space given by (2.12), where the remaining parameters are taken as $C=75$, $k=0.5$, and $\gamma=2$. The parameter values are the same as those used in Ref. 16. In Ref. 16 instability was not found in the quadrant $\Delta\theta>0$. Here, by drawing the curve $f=0$, one may immediately find the instability region in the third quadrant. We confirmed our theoretical result by directly simulating Eqs. (2.1). It is found that the trajectory oscillates as soon as the parameters are forced to cross the boundary and to get into the shaded region. However, outside of the shaded region the trajectory approaches the stationary solution asymptotically. We are interested by the fact that in Fig. 4 the instability region already qualitatively coincides with that predicted by (3.21) though the bistability parameter chosen is not really large. The figure is not affected much by varying γ. We draw the figure only in a half of Δ-θ plane since Eqs. (2.6)–(2.12) are symmetrical against the inverse $\Delta,\theta\rightarrow-\Delta,-\theta$. It is not Eqs. (2.1) themselves but only the instability boundary of their steady solutions that have this symmetry property. Increasing C, the instability boundary is expected to be closer and closer to Eq. (3.21). In Fig. 5 we take $C=500$ and keep k and γ unchanged. The instability boundary for positive Δ is perfectly identical to the approximate result (3.21). As $\Delta<0$, the boundary differs from (3.21) significantly. The reason is that with negative Δ the function f does not take the minimal value at the turning point. In region B, a segment of the upper branch loses stability while f at the turning point is still positive, and then the part of the upper branch near the turning point is still stable.

The same discussion can be carried out to the lower branch. However, by a careful calculation we find out that in the leading order the function f vanishes identically. Thus it is necessary to proceed to the next-to-leading order. The calculation becomes a bit longer. Instead of showing the detail of the calculation we directly display some results in Table I, and only remark that the instability boundary in domain "5" is rather different from those predicted by "3" and "4" in Table I.

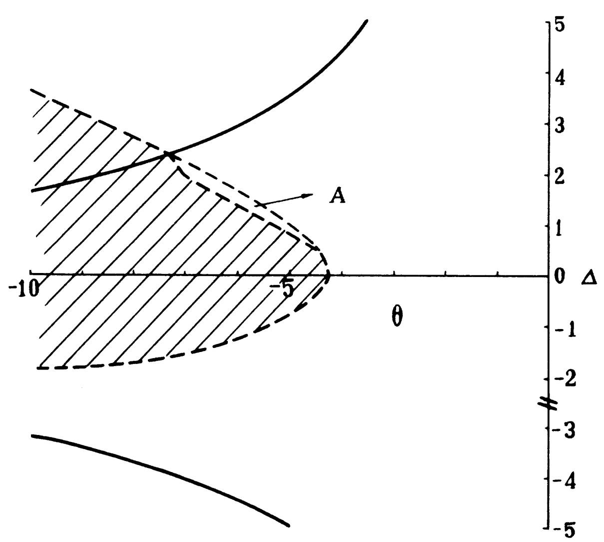

FIG. 4. OB; parameters used are $C=75$, $k=0.5$, and $\gamma=2$. Between the two full curves triple-valued solutions exist. In the hatched region one can observe positive-slope instability. The dotted curve is drawn according to (2.11). In strip A, negative f falls into the negative-slope region.

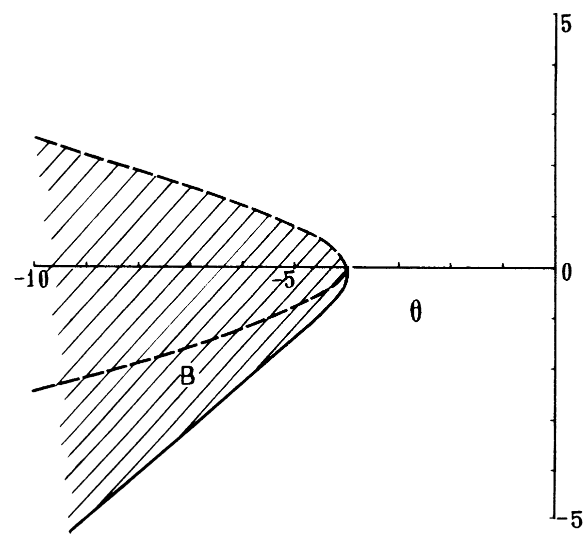

FIG. 5. Same as Fig. 4 with $C=500$. In the hatched region a segment of the upper branch is unstable. On the left of the dotted curve, which coincides with (3.21) very well, the turning point of the upper branch has negative f and loses stability. In region B, an unstable island appears in the upper branch while the part near the turning point is still stable because of positive f.

IV. INSTABILITY OF LIS

Now we should take into account Eqs. (2.6a) and (2.14). First, we prefer to study the simplest nonmistuning case.

A. $\Delta=\theta=0$

As in the case of OB, we may separate the linearizations of (2.13) into two independent sets of equations,

$$\begin{bmatrix} \delta\dot{x} \\ \delta\dot{p} \\ \delta\dot{D} \end{bmatrix} = \begin{bmatrix} -k & -2kC & 0 \\ D_s & -1 & x_s \\ -\gamma p_s & -\gamma x_s & -\gamma \end{bmatrix} \begin{bmatrix} \delta x \\ \delta p \\ \delta D \end{bmatrix} \tag{4.1}$$

and

$$\begin{bmatrix} \delta\dot{\bar{x}} \\ \delta\dot{\bar{p}} \end{bmatrix} = \begin{bmatrix} -k & -2kC \\ D_s & -1 \end{bmatrix} \begin{bmatrix} \delta\bar{x} \\ \delta\bar{p} \end{bmatrix} . \tag{4.2}$$

The first set describes the linear dynamics in real variable space while the imaginary parts of x and p are evolved by the second set. Unlike OB, now the second set of equations can be unstable if

$$x_s^2 < 2C - 1 . \tag{4.3}$$

A direct calculation shows that in the segment

$$0 < x_s^2 < \max(g_1, g_2) , \tag{4.4}$$

$$g_1 = [(C^2+4C)^{1/2} - 2C]/2 ,$$

$$g_2 = \{[(k+\gamma)^2 + 8k\gamma C]^{1/2} - (k+\gamma)\}/(2\gamma) , \tag{4.5}$$

the first set loses its stability. g_1, g_2 come from the conditions $b_3 < 0$ and $f < 0$, respectively [cf. Eq. (3.3)].

If $2C < 1$, we have a unique stable solution. As $2C > 1$, there exist three branches of solutions, the lower branch $(0 < x_s^2 < g_1)$, the upper branch $(2C - 1 < x_s^2)$, and the middle branch $(g_q < x_s^2 < 2C - 1)$. The lower branch and the middle branch are unstable while the upper branch is stable. There is an interesting point worth mentioning. In the part of the middle branch

$$\max(g_1, g_2) < x_s^2 < 2C - 1 ,$$

the steady state is unstabilized by the imaginary set of equations. It means that the phase instability plays an essential role. It does not so in the case of OB.

B. $x^2 \gg 1$

In the limit $x^2 \gg 1$ we recover precisely Eqs. (3.5) and (3.6). It can be concluded that solution (2.14) is stable.

In fact, so far as the stability properties are concerned, LIS is distinguished from OB only by changing the signs of D_s and p_s. Therefore, in all the limits in which D_s and p_s do not play an essential role in (2.6a) and (2.12), the stability properties of LIS must be identical to those of OB. It is the case as $\Delta^2 \gg 1$, $\theta^2 \gg 1$, and $1/C \gg 1$.

In Table II we list the results for various possible asymptotic limits of LIS. The general meaning [$(A, \bar{B})$ means $A \gg B \gg 1$] is the same as in OB. In the limits denoted by "2," the steady solutions are always stable and single valued. By "1" we mean that the solution have the same stability properties as those of $\Delta=\theta=0$. In case of LIS, the regions denoted by 2, are almost the same as in OB. However, in the two cases regions 1 are rather different. For LIS, in the limit where C is much greater than other parameters [$O(1)$], the stability properties are identical to the full resonance case and are not interesting. On the contrary, for OB, the limit $C \gg 1$ produces rich instability bifurcation figures which substantially differ from that of full resonance. On the other hand, in the limits $k \ll 1$ and $\gamma \ll 1$, OB gives rather trivial behaviors "1" and "2," while LIS yield quite interesting instability figures.

TABLE II. Same as Table I for the case of LIS.

	$1/k$	k	$1/r$	r	Δ^2	θ^2	$1/C$	C
$1/k$			3	3	2	2	2	1
k			3	3	2	2	2	1
$1/r$	3	3			2	2	2	1
r	3	3			2	2	2	1
Δ^2	2	3	2	2		2	2	1
θ^2	3	2	2	2	2		2	1
$1/C$	2	2	2	2	2	2		
C	3	4	5	1	2	2		

C. $k \ll 1$

In this limit, Eqs. (2.6a) give rise to

$$a_1 = 2+\gamma, \quad a_2 = (2\gamma + 1 + \Delta^2 + \gamma x^2) ,$$

$$a_3 = \gamma(1+\Delta^2+x^2) ,$$

$$a_4 = [2\gamma(1+\Delta^2+x^2) - 4\gamma C(1+\Delta^2)/(1+\Delta^2+x^2)]k , \tag{4.6}$$

$$a_5 \propto \gamma k^2 ,$$

which reduce (2.11) to

$$f = (a_1 a_2 - a_3) a_3 a_4 \propto a_4 . \tag{4.7}$$

The stable region can be specified by

$$2C < (1+\Delta^2+x^2)^2/(1+\Delta^2) \tag{4.8}$$

The following regions may be proved to be connected:

$$x^2 \gg 1 \to x^2, \quad \Delta^2 \gg 1 \to \Delta^2 \gg 1 \to \Delta^2 \gg 1 ,$$
$$k \ll 1 \to k \ll 1, \quad (1+\Delta^2+x^2) > 2C , \tag{4.9}$$

and then all these regions are stable. Therefore, Eq. (4.8) is not only the necessary condition but also the sufficient condition for the given positive-slope solution to be stable. Moreover, as

$$2C < 1+\Delta^2 , \tag{4.10}$$

the entire branches of positive-slope solutions must be stable; then the laser in absence of injected field is below threshold and the stable segment in the lower branch extends itself to $x^2=0$.

The equations

$$d(a_5)/d(x^2)=0 \tag{4.11a}$$

and

$$a_5=0 \tag{4.11b}$$

give a critical condition for the state equations to be triple valued. Solving x^2 from (4.11a), and inserting it into (4.11b), we may, finally, solve C_b from (4.11b) in terms of Δ and θ. Whenever the condition

$$(1+\Delta^2)/2 > C > C_b \tag{4.12}$$

is satisfied, a full hysteresis loop can be found. The conclusion has been confirmed in Fig. 6, where $C=20$, $k=0.1$, and $\gamma=0.01$. The full curve gives the boundary below which triple-valued solutions exist. The dotted line shows the instability boundary; above that positive-slope solutions turn out to be stable. The figure was drawn according to the theoretical formulas (2.12) and (2.14). It has been perfectly confirmed by directly simulating Eqs. (2.13). In the dashed region we find that both the upper and the lower branches are stable. It is surprising that the stable segment in the lower branch can be extended

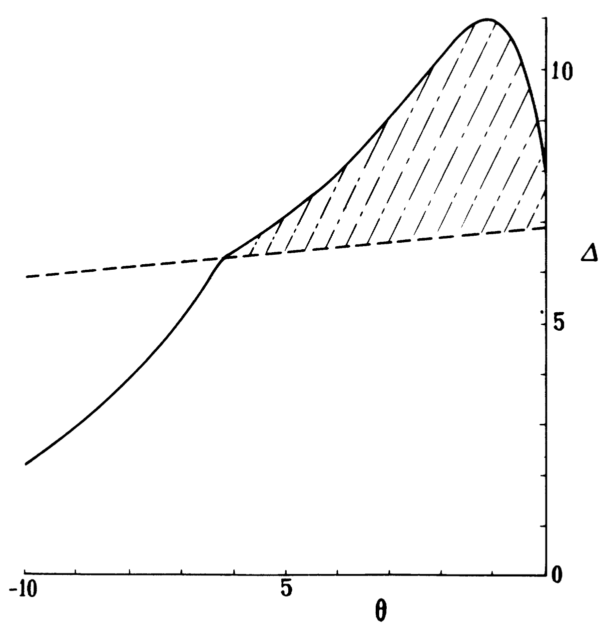

FIG. 6. LIS; parameters used are $C=20$, $k=0.1$, $\gamma=0.01$. Positive-slope instability appears below the dotted line, and triple-valued solutions are available below the solid curve. In the hatched region, bistability and also a full hysteresis loop can be observed. The instability boundary (the dotted line) is approximately provided by (4.10).

down to $x^2=0$. A full hysteresis loop between coexisting stable steady states can be easily found in this parameter domain. The evidence of this domain has never been reported in the literature. An exciting and, possibly, practical interesting discovery by our theory is that a new type of optical switch may be designed in LIS instead of OB. However, to find this bistable domain the combination of parameters should be properly chosen. First, it is easier to find full hysteresis loops in the region $\Delta\theta<0$ than in $\Delta\theta>0$ (in the latter case only a very small bistable region can be found). Second, the atomic detuning must be chosen not too large as well as not too small. In the former case we can not find triple-valued solutions, while in the latter situation the low branch can not be stabilized.

Though the parameter k used in Fig. 6 is not really small, the coincidence between the exact result and the approximate formula (4.10) is already satisfactory. Decreasing k gradually, the instability boundary may be closer and closer to the lines parallel to the θ axis at $\Delta=\pm\sqrt{2C-1}$. An interesting phenomenon is that the instability boundary is not affected by θ and γ as $k \ll 1$. In Table II we represent this kind of stability property by "3."

D. $k \gg 1$

Now we have

$$\begin{aligned} &a_1=2k, \quad a_2=k^2(1+\theta^2) , \\ &a_3=k^2(1+\theta^2)(\gamma+2)-2k^2C(1+\Delta^2)/(1+\Delta^2+x^2) , \\ &a_4=k^2(1+\theta^2)(2\gamma+1+\Delta^2+\gamma x^2)+4k^2CD(1-\Delta\theta) \\ &\qquad +4\gamma k^2CD+2\gamma k^2C(1+\Delta\theta)x^2/(1+\Delta^2+x^2) \\ &\qquad +4k^2C^2D^2 , \\ &a_5 \propto \gamma k^2 , \end{aligned} \tag{4.13}$$

and

$$f=a_1a_2(a_3a_4-a_2a_5) \propto a_3a_4-a_2a_5 . \tag{4.14}$$

It is not difficult to analyze (4.14) thoroughly. Nevertheless, in the present paper we restrict ourselves to the simplest cases. We may further simplify (4.14) by the following auxiliary limits.

1. $k \gg \gamma \gg 1$

Then we obtain the stability condition as

$$\begin{aligned} f&=a_1a_2a_3a_4 \\ &\propto a_4 \\ &=\gamma k^2(1+\theta)^2(2+x^2) \\ &\qquad +4\gamma k^2CD+2\gamma k^2C(1+\Delta\theta)x^2/(1+\Delta^2+x^2)>0 , \end{aligned} \tag{4.15}$$

leading to

$$\begin{aligned} x^2(1+\Delta\theta) < -[&(1+\theta^2)(2+x^2)(1+\Delta^2+x^2) \\ &-4C(1+\Delta^2)]/(2C) . \end{aligned} \tag{4.16}$$

In the case of $\Delta=0$, all the positive-slope solutions (from $x^2=0$) may be stabilized if the bistability parameter C satisfies

$$C<(1+\theta^2)/2 . \tag{4.17}$$

2. $k \gg 1/\gamma \gg 1$

In this case we have

$$4k^2C(1+\Delta^2)/(1+\Delta^2+x^2)<2k^2(1+\theta^2) . \tag{4.18}$$

Under the condition

$$2C<(1+\theta^2) , \tag{4.19}$$

positive-slope instability can never emerge, and then optical bistability may be expected in the domain $(1+\theta^2)/2>C>C_b$, with C_b being provided in Eqs. (4.11). This type of stability behavior is denoted by "3" since the stability properties in this region is similar with that of the region $k \ll 1$. Numerical results confirm (4.19). In Fig. 7 we choose $k=200$, $C=20$, and $\gamma=0.01$. In the dashed region triple-valued solutions exist and both the upper and lower branches are stable. A full hysteresis can be justified by directly solving the time-dependent solution of the differential equations (2.13).

3. $k \gg C \gg 1$

To make the calculation more compact we assume that both the upper branch and lower branch may be destabilized first from the turning points. These assumptions are verified by many numerical examples. Of course, they are not always true. Nevertheless, here we simply use these assumptions without specifying the conditions under which the assumptions are valid.

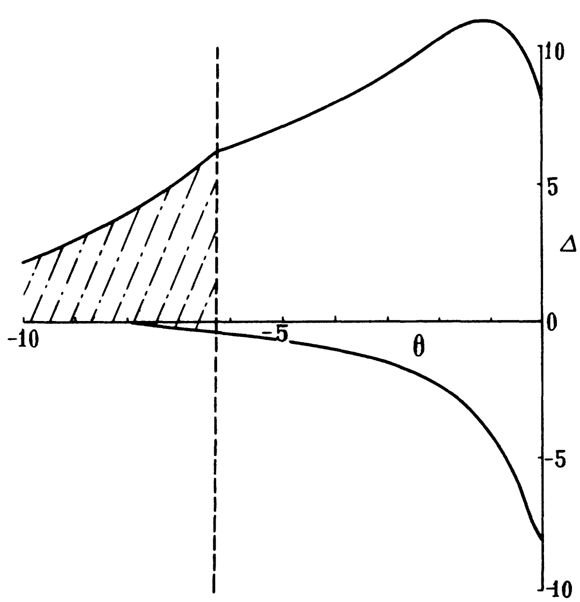

FIG. 7. Same as Fig. 6 with $k=200$. Now Eq. (4.19) is represented by the dotted line. In the hatched region, the entire lower and upper branches are stable, and a full hysteresis loop can be realized.

In the upper branch the condition for the turning point to be unstable reads

$$f \propto a_3a_4 \\ =2\gamma k^2C\{(1+\theta^2)(2+\gamma)-2[(1+\Delta^2)(1+\theta^2)]^{1/2}\} \\ \times\{[(1+\Delta^2)(1+\theta^2)]^{1/2}+(1+\Delta\theta)\} \tag{4.20}$$

where we apply Eq. (3.8). The coefficient a_4 is definitely positive. Thus the sign of f is determined uniquely by that of a_3. Finally, the instability boundary of the upper branch is specified by

$$1+\Delta^2=(1+\theta^2)(1+\gamma/2)^2 . \tag{4.21}$$

Comparing Eq. (4.21) with (3.21), we find that Δ θ completely alter their positions. In (3.21) of OB, the system can be destabilized by increasing θ^2 while stabilized by increasing Δ^2 for a given θ. Now in (4.21) of LIS, the behavior is completely the opposite. We denote this instability boundary by "4" in Table II.

As $k \gg C \gg 1$, the entire lower branch must be unstable because of the fact that a_3 as well as f must be negative.

E. $\gamma \ll 1$ and $\gamma \gg 1$

As the limit $\gamma \ll 1$ is taken, we obtain from (2.6a)

$$a_1=2k+2, \quad a_2=k^2(1+\theta^2)+(1+\Delta^2)+4kCD+4k , \\ a_3=2k(1+\Delta^2)+2k^2(1+\theta^2)+4kCD(k+1) , \\ a_4=k^2(1+\theta^2)(1+\Delta^2)+4k^2CD(1-\Delta\theta)+4k^2C^2D^2 , \\ a_5 \propto \gamma k^2 . \tag{4.22}$$

According to Eq. (2.12) and the limit $\gamma \ll 1$, we have

$$f=a_3a_4(a_1a_2-a_3)-(a_1a_4)^2 . \tag{4.23}$$

Now all the previous calculations can be repeated. However, here we only give the results.

1. $1/\gamma \gg 1/k \gg 0$

The instability boundary is determined by the sign of a_3,

$$2C=(1+\Delta^2+x^2) ,$$

which is the same as (4.10).

2. $1/\gamma \gg k \gg 1$

Again, the instability boundary is related to the sign of a_3. The criterion reads

$$2C=(1+\theta^2)(1+\Delta^2+x^2)/(1+\Delta^2) ,$$

which is nothing but (4.18).

3. $1/\gamma \gg C \gg 1$

The entire lower branch must be unstable because of a_2 and a_3; that is not interesting to us. However, the stability properties of the upper branch is unusual. Controlling the parameter properly, it may be found that the segment near the turning point is stable while in the upper branch an unstable island exists. It can be seen in Fig. 3. In Table II we denote this domain by "5."

In the limit $\gamma \gg 1$, Eqs. (3.17) and (3.18) can be used to test the stability properties of the system by altering the signs of D and p. Finally, the results are the following.

4. $\gamma \gg 1/k \gg 1$

The sign of the function f is identical to the sign of a_4, and then the stability properties of the steady state is described by Eq. (4.10).

5. $\gamma \gg k \gg 1$

It can be verified that altering the limiting orders $k \gg \gamma \gg 1$ by $\gamma \gg k \gg 1$ does not change the stability properties of the state. Therefore, the instability boundary in the present case is given by Eq. (4.16).

V. CONCLUSION

The main achievement in the presentation is the derivation of the instability criterion (2.12). With this criterion we have the potential capacity to study the global structure of instability regions by an analytical method which may be much more convenient than the approaches used before. In principle, the basin structure of the well-behaved function f, i.e., the global structure of the instability domains of OB and LIS, can be analytically studied without resorting to any asymptotic limit, though in the present paper we consider only various limiting cases.

In this presentation we unify the discussions of OB and LIS in various possible asymptotic limits, of which some are analyzed previously in separate publications and by different procedures. By listing the results of all possible limits we may get general ideals about instability regions in the parameter space. In both OB and LIS we reveal five distinct regions where the steady state has diverse stability properties. It is expected that these regions revealed in the limiting cases can be extended to the domain where various parameters have finite and practical values. This possibility has been confirmed by Figs. 4–7.

Though throughout the paper we perform only the simplest discussions rather than general complicated calculations, some interesting results have been already manifested. In OB it seems that for the lower branch to be unstable both atomic and cavity detunings should be nonzero ($\Delta\theta > m$, m is a certain positive number) while for the upper branch to be unstable a large enough cavity mistuning is required (then one may destabilize the system by raising θ). In the case of LIS, we find, for the first time, some regions where a full hysteresis loop can be realized.

The approach has a very wide application. For instance, it can be easily applied to OB and LIS with multiphoton processes, and the systems where more than one mode is involved. Moreover, the application of the approach to maser systems is direct, and we expect that this application may lead to remarkable new results.

[1]M. Gibbs, S. L. McCall, and T. N. C. Venkatesan, Phys. Rev. Lett. **36**, 1135 (1976).

[2]J. V. Moloney, H. M. Gibbs, and F. A. Hopf, in *Proceedings of the Topical Meeting on Optical Bistability, Rochester, NY, 1983,* edited by C. M. Bowden, H. M. Gibbs, and S. L. McCal (Plenum, New York, 1984).

[3]M. B. Spencer and W. E. Lamb, Jr., Phys. Rev. A **5**, 884 (1972).

[4]S. Blit, U. Ganiel, and D. Treves, Appl. Phys. **12**, 69 (1977).

[5]K. Ikeda, H. Daido, and O. Akimoto, Phys. Rev. Lett. **45**, 709 (1980).

[6]H. Haken, Phys. Lett. **53A**, 77 (1975).

[7]M. Mayr, H. Risken, and D. Vollmer, Opt. Commun. **36**, 480 (1981).

[8]L. A. Lugiato, Lett. Nuovo Cimento **33**, 609 (1978).

[9]L. A. Lugiato, L. M. Narducci, D. K. Bandy, and C. A. Pennise, Opt. Commun. **46**, 64 (1983).

[10]T. Yamada and R. Graham, Phys. Lett. **53A**, 77 (1975).

[11]M. J. Scholz, T. Yamada, H. Brand, and R. Graham, Phys. Lett. **82A**, 321 (1981).

[12]R. Bonifacio and P. Meystre, Opt. Commun. **29**, 131 (1979).

[13]V. Benza and L. A. Lugiato, Lett. Nuovo Cimento **26**, 405 (1979).

[14]P. D. Drummond, Opt. Commun. **40**, 224 (1982).

[15]F. A. Hopf, P. Meystre, P. D. Drummond, and D. F. Walls, Opt. Commun. **31**, 245 (1979).

[16]L. A. Lugiato, R. J. Horowicz, and G. Strini, Phys. Rev. A **30**, 1366 (1984).

[17]L. A. Lugiato and L. M. Narducci, Phys. Rev. A **32**, 1576 (1985).

[18]T. Erneux and P. Mandel, Phys. Rev. A **28**, 896 (1983).

[19]T. Erneux and P. Mandel, Phys. Rev. A **33**, 1777 (1986).

[20]L. A. Lugiato, L. M. Narducii, D. K. Bandy, and C. A. Pennise, Opt. Commun. **43**, 281 (1982).

[21]H. Haken, *Synergetics: An Introduction* (Springer, New York, 1983).